Supplementary sections and figures

The muscle fiber type-fiber size paradox: hypertrophy or oxidative metabolism?

Contents **page**

Supplementary section I: qPCR analysis 2

Supplementary section II: SDH activity and total actin mRNA content 4

Supplementary Figure 1 6

Supplementary Figure 2A 7

Supplementary Figure 2B 8

Supplementary Figure 2C 9

Supplementary Figure 2D 10

Supplementary Figure 2E 11

Supplementary section I – qPCR analysis

Animals and tissue preparation
This study was performed in accordance with the guidelines and regulations concerning animal welfare of the Dutch law and approved by the Committee of Ethics of animal experimentation at the VU University Amsterdam. Six adult male Wister rats, weighing 386 ± 11 (mean ± SD) g, were sedated with isoflurane and the heart was removed. After that, soleus (SO) and extensor digitorum longus (EDL) muscles, weighing 124 ± 11 mg and 168 ± 13 (mean ± SD) mg respectively, were dissected from the left leg, snap-frozen and stored at -80 ºC for later analysis.

Total RNA isolation. Total RNA was extracted from the muscles using the RiboPure kit (Applied Biosystems) according to the manufacturer's instructions. RNA concentrations were determined in duplo by spectroscopy (ND-1000 spectrophotometer; Nanodrop Technologies, Wilmington, DE). RNA purity was ensured by 260/280 ratio (range 2.00-2.11, mean 2.04). The muscle total RNA concentration was calculated on the basis of total RNA yield (μg) per weight (mg) of the analyzed sample (Fig. 2A).

Reverse Transcription (RT). Five hundred nanograms of total RNA per muscle were reverse transcribed using the high capacity RNA-to-cDNA kit (Applied Biosystems) containing random primers in a 20 μl total reaction volume. Tubes were heated at 25 ºC for 5 min, followed by 42 ºC for 30 min. Finally the tubes were heated to 85 ºC for 5 min to stop the reaction and stored at -80 ºC until used in the qPCR reaction.

qPCR. A quantitative PCR analysis method was applied to study the expression of 18S RNA and mRNAs of α-skeletal actin, glyceralde-3 phosphate dehydrogenase (GAPDH), insulin-like growth factor-I (all isoforms), muscle ring finger-1 (MuRF1), muscle atrophy F-box (MAFbx) and myostatin. The sequences for the primers (Invitrogen, The Netherlands) used for the specific RNA and mRNA targets are shown in Table 1. For each target, RT and PCR reactions were carried out under identical conditions by using the same reagent premix for all samples. Five microliter of each RT reaction was used for the PCR amplification. cDNA dilutions were set so that both the target mRNA and 18S product yields were in the linear range of the semi-log plot when the yield is expressed a function of the number of cycles. Amplifications were carried out in a StepOne real-time PCR machine (Applied Biosystems) with an initial activation/denaturing step of 23 s at 95 ºC followed by an annealing step of 30 s at 60 ºC. The range of cycle threshold values was 15-30. Specificity was confirmed by melting curve analysis after amplification. 18S RNA and mRNA data were normalized to total RNA yield per sample (Fig. 2B) as well as to the weight of tissue needed for extracting the amount of RNA used for cDNA synthesis (Fig. 2C). Differences in mRNA for each primer are shown relative to EDL.

Statistics. For each muscle, three samples were included. All values are reported as mean values ± SEM. Differences between muscles in total RNA per muscle tissue weight and in mRNA target were determined with independent t-tests relative to the EDL value, which was set to 1.

Table 1: sequence of the specific primers used in the quantitative PCR analyses

Target mRNA	PCR primer sequence 5'→ 3'
18S RNA	Forward: CGAACGTCTGCCCTATCAACTT
	Reverse: ACCCGTGGTCACCATGGTA
α-skeletal actin	Forward: CGACATCGACATCAGGAAGGA
	Reverse: GGTAGTGCCCCCTGACATGA
GAPDH	Forward: TGGCCTCCAAGGAGTAAGAAAC
	Reverse: GGCCTCTCTCTTGCTCTCAGTATC
IGF-I (all isoforms)	Forward: CCTACAAAGTCAGCTCGTTCCA
	Reverse: TCCTTCTGAGTCTTGGGCATGT
MAFbx	Forward: TGAAGACCGGCTACTGTGGAA
	Reverse: CGGATCTGCCGCTCTGA
MuRF1	Forward: TGCCCCCTTACAAAGCATCTT
	Reverse: CAGCATGGAGATGCAATTGC
myostatin	Forward: GTTCCCGGAGAGACTTTGG
	Reverse: CGACAGCACCGCGATTC

GAPDH: glyceralde-3 phosphate dehydrogenase, MuRF1: muscle ring finger-1, MAFbx: muscle atrophy F-box.

Supplementary section II – Correlation between succinate dehydrogenase (SDH) activity and total actin mRNA content in Xenopus laevis muscle fibers.

Animals and tissue preparation

For the determination of the relationship between SDH activity and the actin mRNA expression we used two female *Xenopus laevis* (10 cm in body length). Treatment of animals was in accordance with the guidelines and regulations concerning animal welfare and experimentation set forth by Dutch law, and approved by the Committee on Ethics of Animal Experimentation at the VU University, Amsterdam. After maintaining the animals in ice water for about 10 minutes, they were killed by decapitation. Subsequently, iliofibularis muscles were excised, stretched passively to just over slack length and kept for half an hour in oxygenated Ringer's solution (mM: NaCl, 116.5; KCl, 2.0; $CaCl_2$, 1.9; NaH_2PO_4, 2.0; EGTA, 0.1; pH 7.2) at room temperature (RT; 22 ± 1 ºC). After this, muscles were frozen in liquid nitrogen and prepared for cryostat sectioning. For staining of SDH activity and in situ hybridization, serial sections (16 and 10 µm thick, respectively) were cut from the middle region of the muscle and mounted on glass slides, coated with Vectabond (Vector Laboratories, Burlingame, CA) and treated with diethyl pyrocarbonate (DEPC), and air-dried. Chemicals were purchased from Sigma-Aldrich unless state otherwise.

Succinate dehydrogenase (SDH) activity

SDH activity was determined according to references (1, 3). After cutting, muscle cross-sections (16 µm thick) were air-dried for 15 min and incubated for SDH activity in a medium consisting of 37.5 mM sodium phosphate buffer, pH 7.6, 75 mM sodium succinate, 5 mM sodium azide and 0.4 mM tetranitro blue tetrazolium, in the dark at 20 °C for 45 minutes. The reaction was stopped in 10 mM HCl and the sections were washed in water, embedded in glycerin gelatin and stored at 4 ºC. The absorbance of the final reaction product was measured at 660 nm (A_{660}) and was converted to the rate of staining, expressed as absorbance units per µm section thickness (see below).

In Situ Hybridization for actin mRNA

After cutting and drying, sections (10 µm thick) were stored in slide boxes at -80°C until analysis. The probe for detection of all actin isoforms (cardiac, skeletal and cytoskeletal actin) was amplified from Xenopus laevis embryos cDNA using forward primer 5'- CAGCACCAGCTCTCCTGTGCTA-3' and the reverse primer 5'- TCTCAAAGTCCAAAGCCACATA-3' (Eurogentec, Belgium) directed against the N-terminal coding region (721 bp, 11-732 nt, gene ID X03469) (2).

The PCR product was cloned into vector pGEMT (Promega, France). Digoxigenin(DIG)-labeled antisense and sense RNA probes were produced by in vitro transcription using RNA labeling mix (Roche Diagnostics Research, The Netherlands) according to the manufacturer's instructions. After the labeling reaction, the probe was dissolved in DEPC treated water and its concentration was measured (ND-1000 spectophotometer; Nanodrop Technologies, Wilmington, DE).

Frozen sections were air dried and fixed in 4% paraformaldehyde solution (in PBS) for 20 minutes at 20 °C and washed in PBS. The sections were then treated with proteinase K (10µg/ml) for 20 minutes at 20 °C, washed 2 times 3 minutes in PBS and fixed in a 4% formaldehyde solution for 5 minutes, where after the sections were incubated in tri-ethanolamine solution (1.33% TEA, pH 8.0) for 5 minutes and tri-ethanolamine with acetic anhydride (TEA solution + 100 µl acetic anhydride) for 5 minutes. After TEA incubation, slides were washed 2 times for 3 minutes and slides were incubated for 30 minutes in prehybridization mix [50% formamide, 3 x SCC (20x SCC; 3 M NaCl, 0.3 M tri-sodium citrate, pH 4.5), 1% blocking reagent (Roche Diagnostics Research, The Netherlands), 10 mM EDTA, 1 mg/ml torula mRNA, 2.5 mg/ml 3-[(3-cholamidopropyl)dimethylammonio]-1-propanesulfonate, 0.1 mg/ml heparin, 0.2% Tween-20]. Hybridization was performed in the prehybridization solution with 10mM dithiothreitol (DTT) and the DIG-labeled anti-sense and sense RNA probe at a concentration of 10 ng/µl (total volume 12.5 µl). Sections were hybridized over night at 50 °C in a humidified chamber while covered by Hybri-slips (Sigma-Aldrich).

After hybridization, sections were washed twice with 2x SSC + 0.02% (w/v) sodium dodecyl sulphate (SDS) for 10 minutes at 50 °C, 8 minutes 0.2x SSC + 0.02% (w/v) SDS at 50 °C and 8 minutes 0.2x SSC + 0.02% (w/v) SDS + 10 mM DTT at 50 °C, slides were washed in MAB buffer (10 mM Maleineacid, 150 mM NaCl, pH 7.5) at RT and incubated with sheep anti-DIG Fab fragments conjugated with alkaline phosphatase (1:4000, Roche) in 10% (w/v) heat inactivated sheep serum, 1 % (w/v) blocking reagent, and 0.1% (w/v) Tween-20 in MAB buffer over night at 4 °C.

The sections were washed 5 times 15 minutes at RT in MAB buffer and incubated for 3 minutes in AP buffer (0.1 M NaCl, 0.1 M TRIS HCl, 50 mM $MgCl_2$, 0.1 % (w/v) Tween-20) supplemented with levalisol (Vector Laboratories, UK; final concentration 1 mM). Chromogenesis was performed in the dark using 1 mM levamisol in BM purple (Roche) for 50 hours at 20 ºC. Finally, the sections were mounted in glycerine gelatine and stored at 4 ºC. Sense probes were used to determine the level of non-specific probe binding. The absorbance of the final reaction product was measured at 550 nm (A_{550}) and expressed as absorbance units.

Microdensitometry

The absorbance values of the final reaction products in the sections were determined using a Leica DMRB microscope (Wetzlar, Germany) fitted with calibrated grey filters using different interference filters. Absorbances for SDH, and actin mRNA were determined at 660 nm (A_{660}) and 550 nm (A_{550}), respectively. Images were recorded with a ×20 objective and a Sony XC-77CE camera (Towada, Japan) connected to an LG-3 frame grabber (Scion, USA) in an Apple Power Macintosh computer. Recorded images were analyzed with the public domain programme NIH-Image V1.61 (US National Institutes of Health, available at http://rsb.info.nih.gov/nih-image/). Grey values were converted to absorbance values per pixel using the grey filters and a third-degree polynomial fit in the calibrate option of NIH-image. Morphometry was calibrated using a slide micrometer and the set scale option in NIH-image, taking the pixel-to-aspect ratio into account.

References

1. **Pool CW, Diegenbach PC, and Scholten G.** Quantitative succinate-dehydrogenase histochemistry. I. A Methodological study on mammalian and fish muscle. *Histochemistry* 64: 251-262, 1979.
2. **Stutz F and Spohr G.** Isolation and characterization of sarcomeric actin genes expressed in Xenopus laevis embryos. *J Mol Biol* 187: 349-361, 1986.
3. **van der Laarse WJ, Diegenbach PC, and Elzinga G.** Maximum rate of oxygen consumption and quantitative histochemistry of succinate dehydrogenase in single muscle fibres of Xenopus laevis. *J Muscle Res Cell Motil* 10: 221-228, 1989.

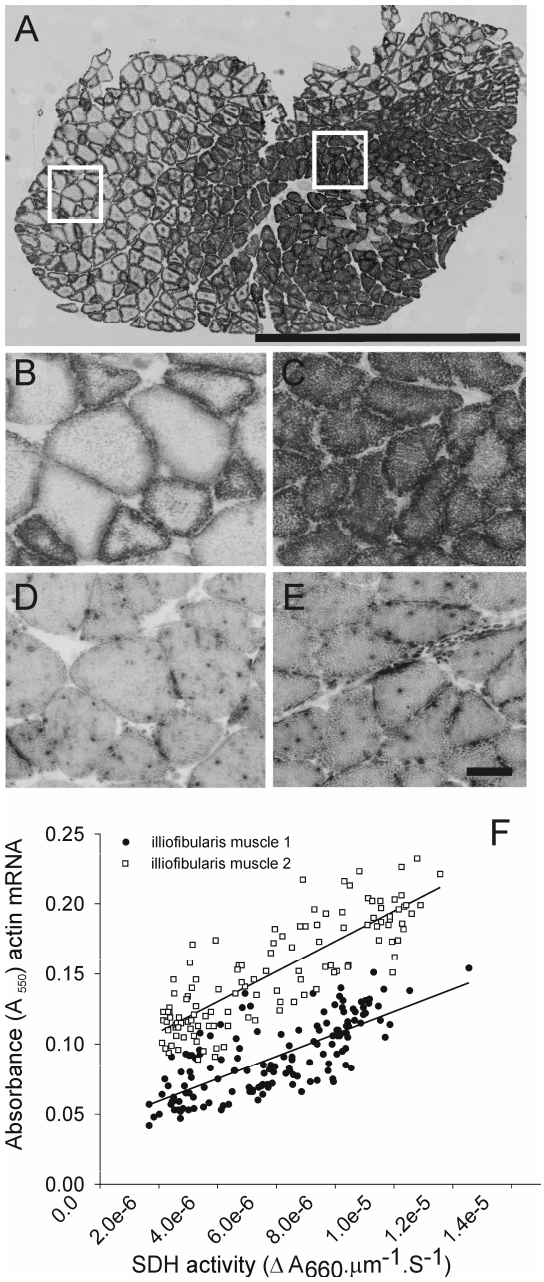

Supplementary Fig 1. Correlation between oxidative metabolism and actin mRNA concentration. **A**) Overview of a whole muscle section of the Xenopus laevis iliofibularis muscle stained for SDH activity. Note the differences in size between the intensively stained high oxidative muscle fibers (type 3 according to the classification for amphibian muscle: Lännergren J and Smith RS. *Acta Physiol Scand* 68: 263-274, 1966.) on the right and the large low oxidative (type 1) muscle fibers on the outside of the muscle. Bar indicates 3 mm. **B** and **C**) Magnifications of the squares indicated in the overview. **D** and **E**) Magnifications of muscles parts stained for actin mRNA (all isoforms) by in situ hybridization (for methods see supplementary section II). Staining is the most intensive in the small type 3 high oxidative muscle fibers on the right side. The outer regions consist of small and large type 1 fibers showing relatively high and low SDH staining, respectively. Note the local intensive actin mRNA staining in the cytoplasm co-localizing with the myonuclei, which for Xenopus muscle are located within the cytoplasm and not subsarcolemmal like in mammalian skeletal muscle. Bar in E indicates 100 µm and is valid for B-E. **F**) Absorbance levels of the actin mRNA staining are related to the SDH activity (for muscle 1 and 2, $r^2 = 0.71$ and 0.54, respectively at $p<0.0001$).

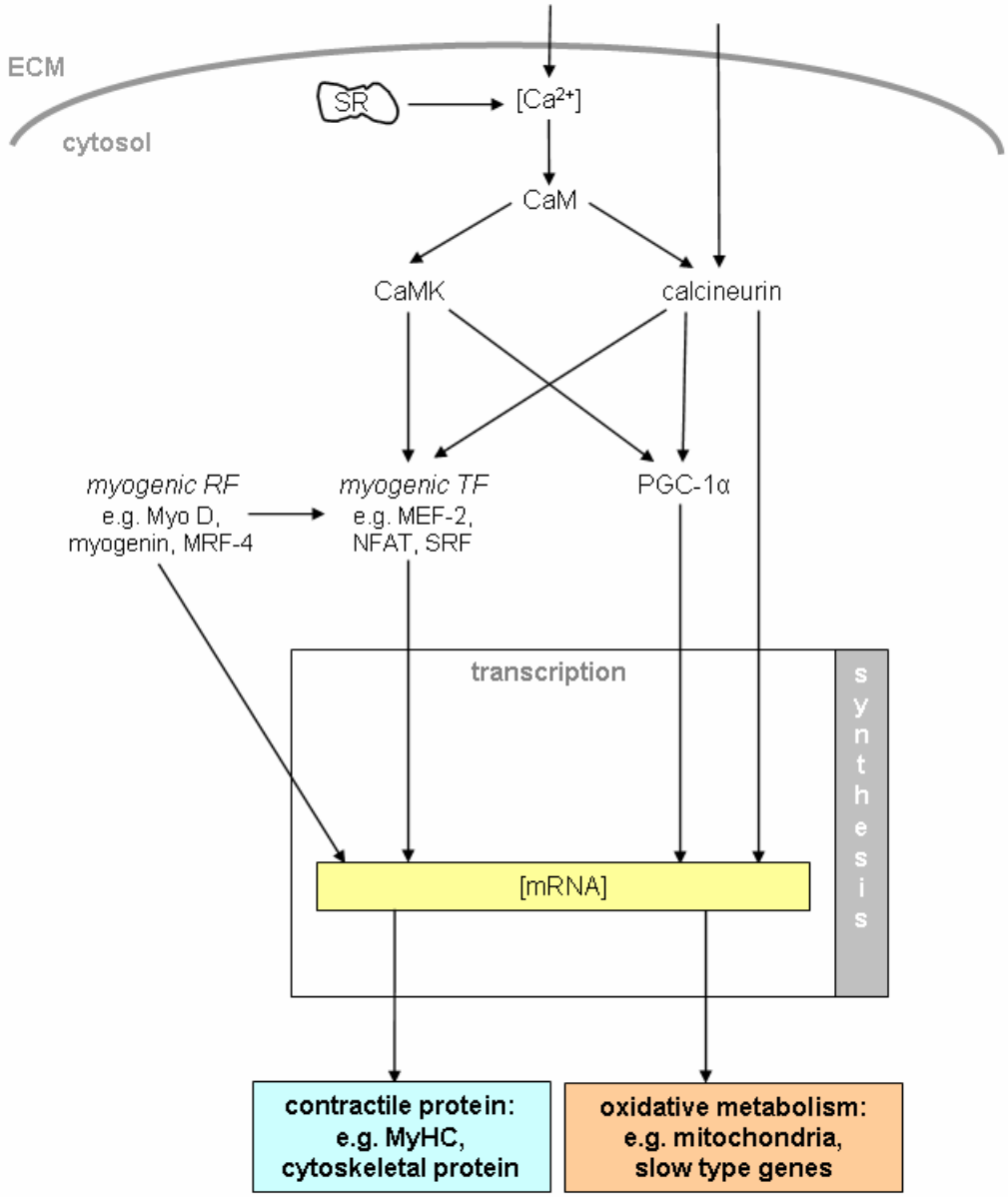

Supplementary Fig. 2A. The Ca^{2+}-calmodulin dependent pathways regulate gene expression in skeletal muscle. Both calcineurin and CaMK are activated in response to changes in $[Ca^{2+}]i$ in a calmodulin-dependent way. Calcineurin and CaMK control several downstream myogenic transcription factors and PGC-1α, which enhance gene expression involved in oxidative metabolism (e.g. slow troponin I, myoglobin), mitochondrial biogenesis and induce fast-to-slow transitions in MyHC isoforms. *Abbreviations: CaM: calmodulin, CaMK: calmodulin-dependent protein kinase, ECM :extracellular matrix, MEF-2: myocyte enhancer factor-2, MyHC: myosin heavy chain, MRF: myogenic regulatory factor, NFAT: nuclear factor of activated T-cells, PGC-1α: peroxisome proliferator-activated receptor γ coactivator-1α, SR: sarcoplasmatic reticulum, SRF: serum response factor, TF: transcription factors.*

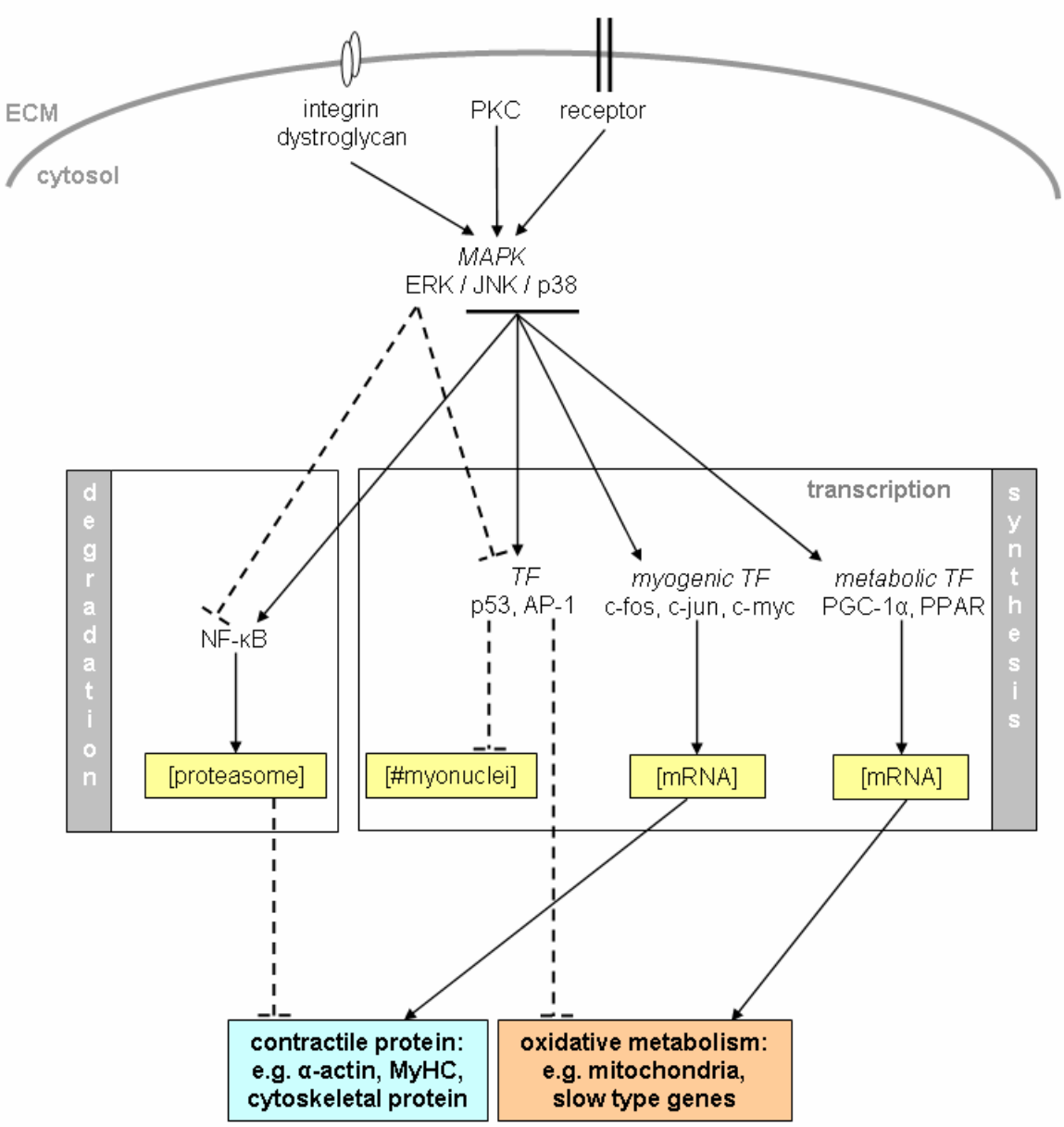

Supplementary Fig. 2B. Figure summarizing the involvement of the mitogen-activated protein kinase (MAPK) pathways in skeletal muscle protein turnover. MAPK activation is mediated by upstream protein kinases that are induced by ligand-receptor binding, PKC or integrins / dystroglycans. Subsequently, MAPKs phosphorylate and activate myogenic and metabolic transcription factors, as well as other kinases, which control downstream signaling pathways affecting synthesis of contractile protein, metabolic protein and the degradation of contractile protein. *Abbreviations: see Suppl. Fig. 2A, AP-1: activator protein-1, ERK: extracellular regulated kinase, JNK: c-Jun N-terminal kinase, NF-κB: nuclear factor-κB, p38: 38kDa stress activated protein kinase, PKC: protein kinase C, PPAR: peroxisome proliferator-activated receptors.*

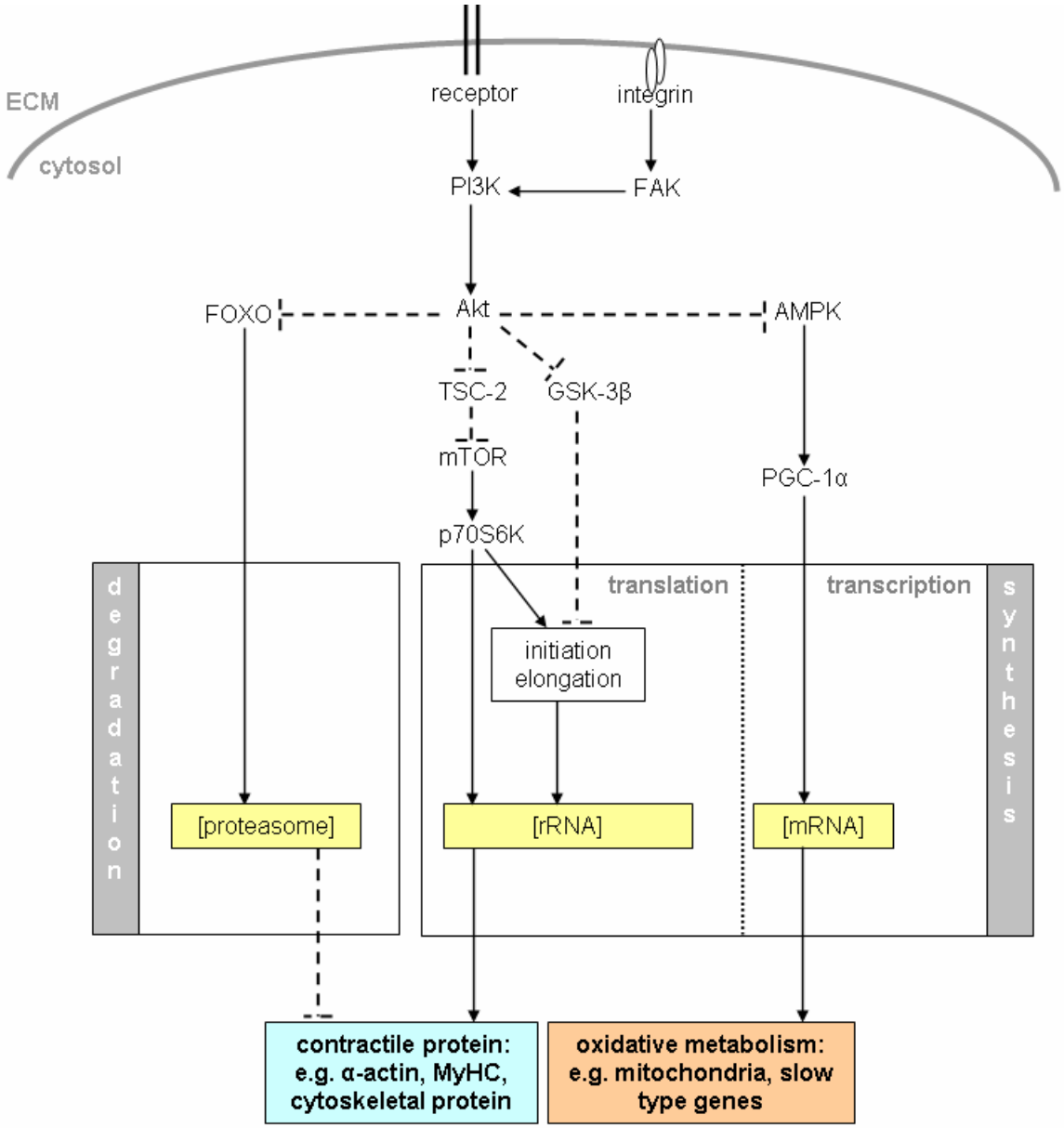

Supplementary Fig. 2C. Signaling pathways involved in inducing hypertrophy. Either receptor binding or integrin-mediated activation of FAK induces activation of PI3K and phosphorylation of Akt. Once activated Akt enhances translation initiation, elongation and ribosomal biogenesis via activation of mTOR and p70S6K as well as via the inactivation of GSK-3β. At the same time Akt inhibits proteasome-mediated degradation of contractile protein via the inhibition of the FOXO family of transcription factors (see Suppl. Fig. 2D). Akt also negatively regulates high oxidative gene expression by inhibiting AMPK (see Suppl. Fig. 2E). In contrast, AMPK inhibits mTOR thereby attenuating translation of mRNA (not shown, see Suppl. Fig. 2E). *Abbreviations: AMPK: AMP-activated protein kinase, FAK: focal adhesion kinase, FOXO: Forkhead box transcription factors O subfamily, GSK-3β: glycogen synthase kinase-3β, mTOR: mammalian target of rapamycin, PI3K: phosphatidylinositol-3 kinase, p70S6K: 70-kDa ribosomal protein S6 kinase, TSC-2: tuberous sclerosis complex-2.*

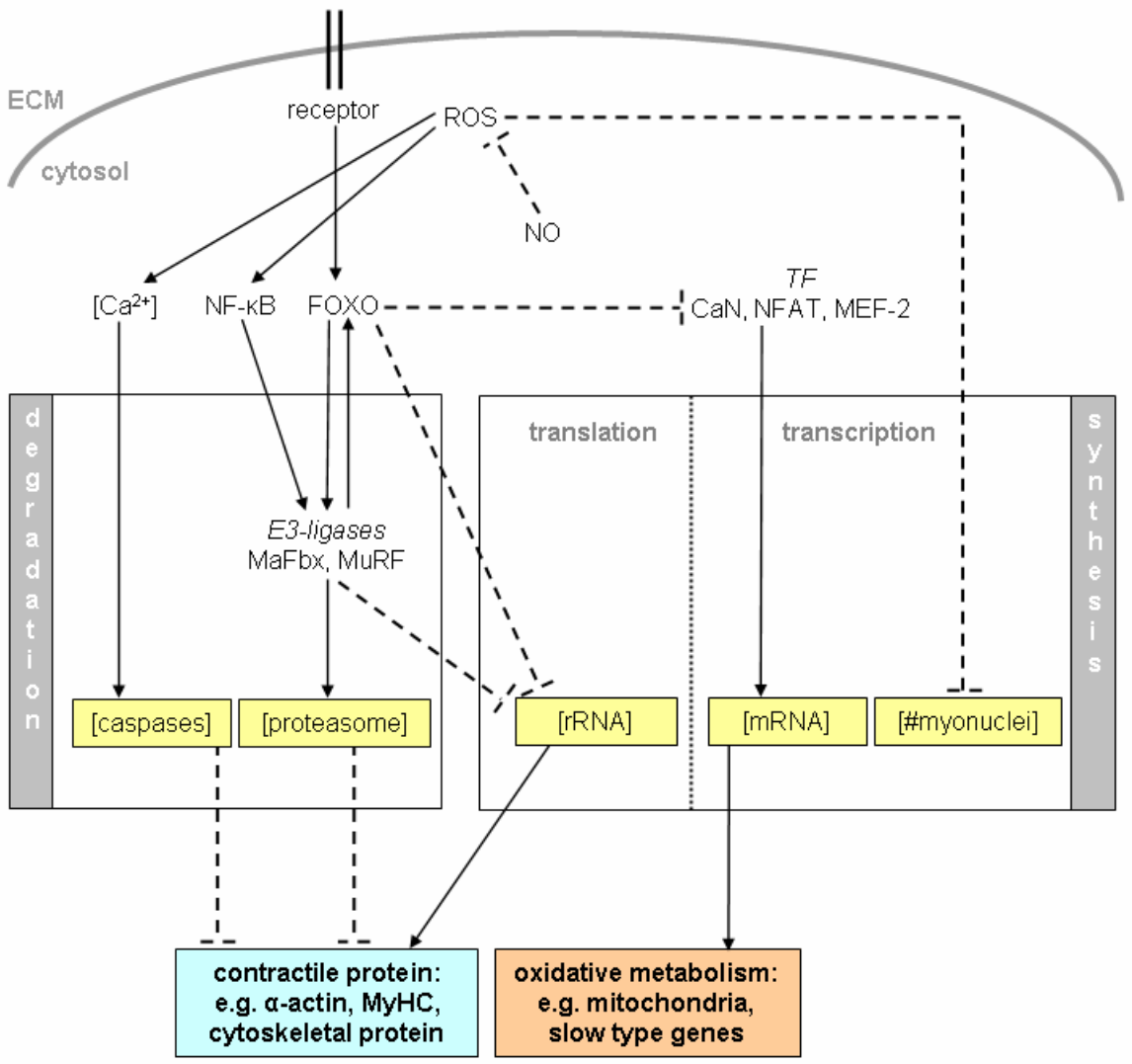

Supplementary Fig. 2D. Pathways involved in enhancing protein degradation and attenuating synthesis during muscle atrophy. FOXO transcription factors up-regulate the expression of E3 ligases (MAFbx and MuRF) and subsequent proteasome activity. The expression of MAFbx prevents the Akt-dependent phosphorylation of FOXO causing FOXO to remain translocated in the nucleus, thereby creating a feed-forward mechanism with FOXO. In addition, FOXO inhibits transcription of slow type genes and both FOXO and the E3 ligases attenuate translation of mRNA into protein. ROS enhance protein degradation via Ca^{2+}-induced caspase activation and via NF-κβ-mediated expression of E3 ligases. In addition, ROS are also involved in myonuclear apoptosis and ROS function can be inhibited by scavengers such as NO. *Abbreviations: see Suppl. Fig. 2A-C CaN: calcineurin, MAFbx muscle atrophy F-box, MuRF: muscle ring finger, NO: nitric oxide, ROS: reactive oxygen species.*

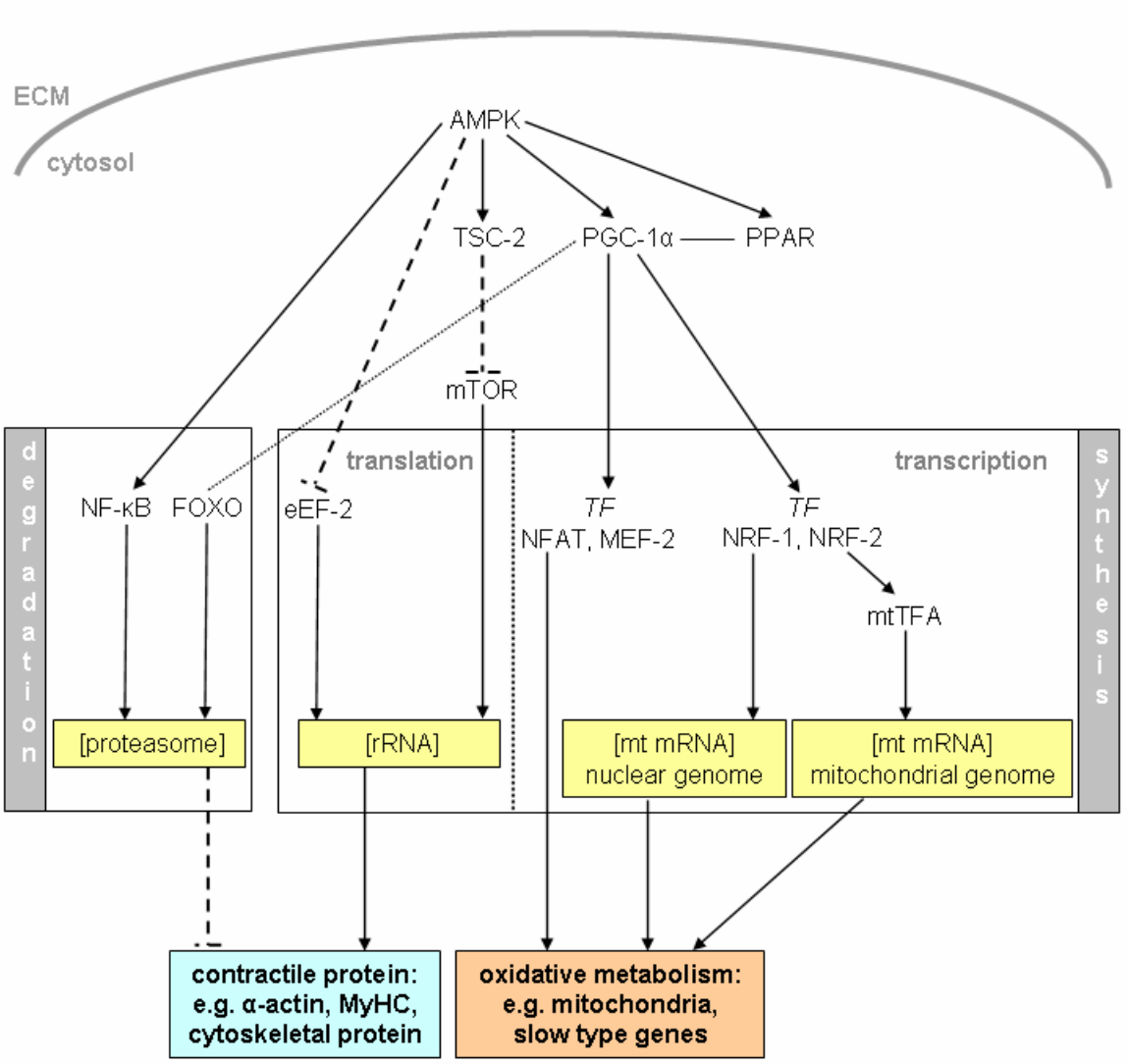

Supplementary Fig. 2E. AMPK mediated pathways involved in skeletal muscle. AMPK-induced expression and activation of PGC-1α and PPAR stimulate gene expression associated with a high oxidative metabolism through several transcription factors that control both myonuclear and mitochondrial genomes. AMPK also attenuates translational processes while at the same time it enhances protein degradation via NF-κβ-mediated proteasome activity (see suppl. fig. 2D) and possibly through PGC-1α-mediated FOXO activity (see text for details). *Abbreviations: see Suppl. Fig. 2A-C, eEF-2: eukaryotic elongation factor-2, mtTFA: mitochondrial transcription factor A, NRF: nuclear respiratory factor.*